

Searching for *s*-Process-Enhanced Metal-Poor Stars

M. A. Cruz^{A,D}, *S. Rossi*^B, and *T. C. Beers*^C

^A Max Planck Institut für Astrophysik, Karl-Schwarzschild-Str. 1, 85748 Garching, Germany

^B Department of Astronomy, Instituto de Astronomia, Geofísica e Ciências Atmosféricas, University of São Paulo, Rua do Matão 1226, Cidade Universitária, São Paulo, 05508-090, Brazil

^C Department of Physics & Astronomy, CSCE and JINA, Michigan State University, East Lansing, MI 48824, USA

^D Corresponding author. Email: mcruz@mpa-garching.mpg.de

Received 2008 November 18, accepted 2009 April 15

Abstract: We present preliminary results for the estimation of barium [Ba/Fe], and strontium [Sr/Fe], abundances ratios using medium-resolution spectra (1–2 Å). We established a calibration between the abundance ratios and line indices for Ba and Sr, using multiple regression and artificial neural network techniques. A comparison between the two techniques (showing the advantage of the latter), as well as a discussion of future work, is presented.

Keywords: surveys — techniques: spectroscopic — stars: abundances

1 Introduction

Metal-poor stars (hereafter, MPS), defined as stars with less than one tenth of the solar iron abundance ($[\text{Fe}/\text{H}] < -1.0$), are important for understanding the chemical enrichment of the early Galaxy. However, the full range of nucleosynthetic pathways for the production of the heaviest elements in such stars is still not fully understood. Additional information on abundance patterns are needed in order to provide clues and constraints on the nature of element production for the first generations of stars.

Many studies of MPS have been carried out in the last decades, making available abundance patterns for stars with metallicities down to almost $[\text{Fe}/\text{H}] = -6$ (Frebel et al. 2008). However, a large fraction of these studies only provide abundance values for elements lighter than iron. Among such studies, the wide-angle spectroscopy surveys, such as the HK survey (Beers, Preston & Shtetman 1985, 1992; Beers et al. 1999), have performed an important role in the identification of numerous low metallicity stars. The aim of the present project is to go one step further and find a method to identify *s*-process-element enhanced MPS, using the available medium-resolution spectroscopy data, and create a pre-selected sample for detailed investigation at higher spectroscopic resolution.

Here we present preliminary results involving two methods for estimation of barium [Ba/Fe], and strontium [Sr/Fe], abundances ratios, discuss the difficulties encountered, and future developments.

2 Data Samples

Our calibration data were selected from the library of medium resolution spectra obtained during the HK (Beers

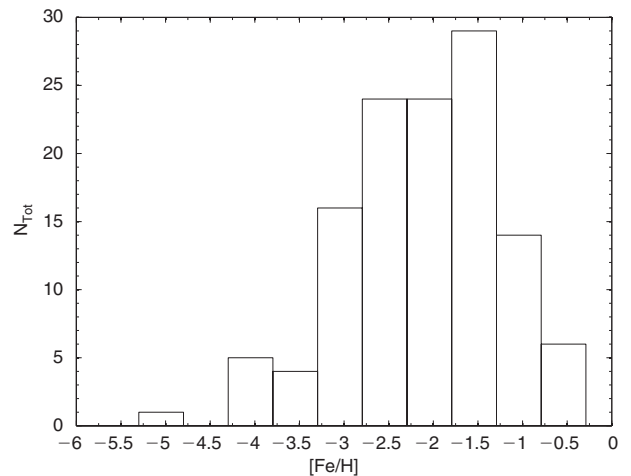


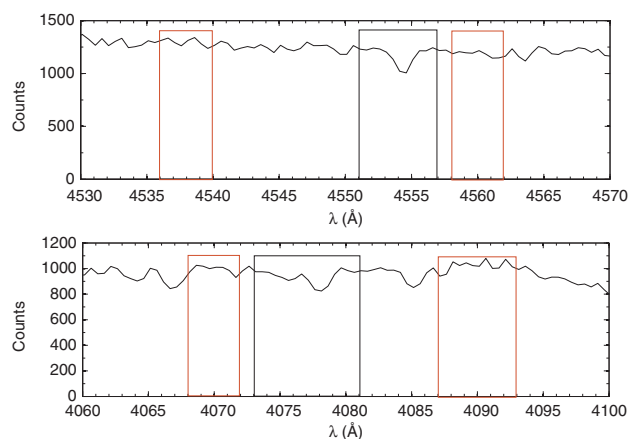
Figure 1 The metallicity distribution function of our calibration sample.

et al. 1985, 1992, 1999) and Hamburg/ESO (Christlieb 2003) surveys with $[\text{Fe}/\text{H}] < -1.0$, and with Ba and Sr abundances ratios already estimated by previous high-resolution studies. Their metallicity distribution (derived from the high-resolution spectra) is shown in Figure 1. We have about 100 spectra with resolution between 1 and 2 Å.

We performed an extensive search for reported abundance ratio values for [Ba/Fe] and [Sr/Fe] in the available literature. Since we found differences from author to author as high as ~ 0.2 dex, we decided to adopt a simple set of selection criteria for the adopted abundances ratios instead of averaging all the values found for a single object, in hopes to decreasing the overall errors.

Table 1. Index definitions

	Ba	Sr
Blue sideband	4536–4540	4068–4072
Line band	4551–4557	4073–4081
Red sideband	4558–4562	4087–4093

**Figure 2** Definition of the indices Ba (top panel) and Sr (bottom panel) in the star LP 625–44. Red boxes are the sidebands and black box is the line band.

The following criteria were applied to the literature sample:

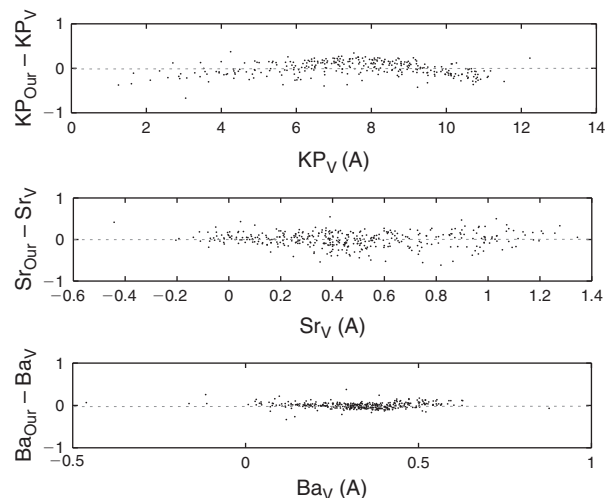
- More recent values, from the nineties (late nineties were preferred) up to the present;
- LTE values;
- Highest S/N and resolving power.

Line indices for barium and strontium were required for the application of our methods, as defined in Table 1 and Figure 2: the Beers et al. (1999) line index (KP) for the CaII K line and the 2MASS¹ (Skrutskie et al. 2006) near-IR colors ($J - K$)₀.

Our program data contains about 35000 stars from the Sloan Digital Sky Survey² Data Release 5 (SDSS, Gunn et al. 1998; York et al. 2000; Adelman-McCarthy et al. 2007). These stars were previously selected by metallicity, using the values of $[Fe/H]$ reported by the SDSS/SEGUE spectroscopic pipeline (Lee et al. 2008a,b; Allende Prieto et al. 2008), have resolving power about $R = 2000$, and cover the wavelength range 3800–9200 Å.

3 Calibration

The line indices were measured using the LECTOR program by Vazdekis et al. (2003), as well as our own code. Figure 3 shows a comparison between the two different methods. The agreement between the two codes is quite good, even for the Sr index which presents a larger scatter. This larger scatter for the Sr index could be explained

**Figure 3** Comparison between the line indices measured with LECTOR and our code.

by two effects: (1) the signal-to-noise ratio in this part of the spectrum: according to Cayrel (1988) the uncertainty in the index is inversely proportional to the S/N ratio thus, the smaller S/N in the Sr location increases the errors; and (2) the continuum placement: the Sr index band is closer to a strong absorption line, which implies more difficulties in the continuum determination. Therefore, the different procedures to estimate the continuum by our and Vazdekis codes could also contribute to the scatter. A quantitative analysis of the errors introduced by continuum determination can be seen in Stetson & Pancino (2008).

Two different procedures were used to perform the calibration: multiple regression and application of an artificial neural network (ANN), as described below.

3.1 Multiple Regression

We have obtained the abundance ratio $[X/Fe]$, where X represents barium or strontium, as a function of $\log_{10}(X)$, $\log_{10}(KP)$ and $(J - K)$ ₀. The regression expressions for barium and strontium are shown below:

$$\begin{aligned}
 [Ba/Fe] = & 7.34(0.02) + 4.37(0.02) \log_{10}(Ba) \\
 & - 3.71(0.03) \log_{10}(KP) \\
 & - 3.15(0.05)(J - K)_0
 \end{aligned} \quad (1)$$

$$\begin{aligned}
 [Sr/Fe] = & 4.59(0.05) + 1.96(0.05) \log_{10}(Sr) \\
 & + 0.04(0.09) \log_{10}(KP) \\
 & - 6.24(0.01)(J - K)_0,
 \end{aligned} \quad (2)$$

where the values in parenthesis are the one sigma errors in the determination of each coefficient.

The standard deviation for the calibration values are about 0.4 and 1.1 dex for barium and strontium, respectively. Therefore, this method is not reliable to measure the strontium abundance ratios, at least by considering the present data. Figure 4 shows the residual values for $[Ba/Fe]$ as a function of the adopted literature values.

¹ Two Micron All Sky Survey.

² <http://www.sdss.org/>.

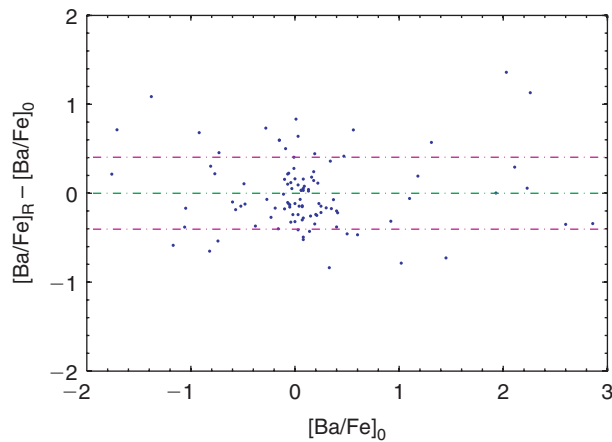


Figure 4 Distribution of the residual of the estimated [Ba/Fe] by regression, as compared to the adopted literature values. The green line represents the mean value of the residual and the pink lines are the 1- σ lines.

4 Artificial Neural Networks

Artificial neural networks (hereafter, ANNs) are playing an increasingly important role in the analysis of large astronomical databases. This technique can be used to find patterns, as well as make predictions (similar to regression). In the latter case, the main advantage over simple regression is the possibility for allowing non-linear interactions of the predictor variables, which can change over the parameter space, in addition to the rapid training and retraining.

For application of the ANN procedure, we have used the same input as in the regression case, e.g., $(Y, X_1, X_2, X_3) = ([X/Fe], \log_{10}(X), \log_{10}(KP), (J - K)_0)$. Since we are conducting a supervised learning exercise, we applied the back-propagation algorithm which propagates backwards the error derivative of the weights, adjusting the weights in order to minimize the final errors of determination. About 80% of the calibration sample were used as a training set, setting aside 20% as a testing set, in a network with 2 layers and 10 nodes. In order to check the ANN's stability, we have used 10 different training and testing subsets.

Figures 5 and 6 show the results for the ANN calibration. It is clear that considerable improvement has been achieved, even for the Sr abundances, in the determination of abundance ratios process. However, there are still problems to be solved in the Sr calibration. As can be seen in the residual plot, there is a small trend with 10–20% error associated (not considering the outlier in the upper left). Since there is no trend when the residual is plotted versus the predictor variables (Sr, *KP* and $(J - K)_0$) and versus the calculated values (see Figures 7 and 8), it is believed that a more homogeneous sample could help solve this problem.

The standard deviation for these calibrations are 0.16 and 0.21 dex for Ba and Sr, respectively.

The primary difficulty in performing such calibrations is related to the gaps in the abundance space. As can be seen

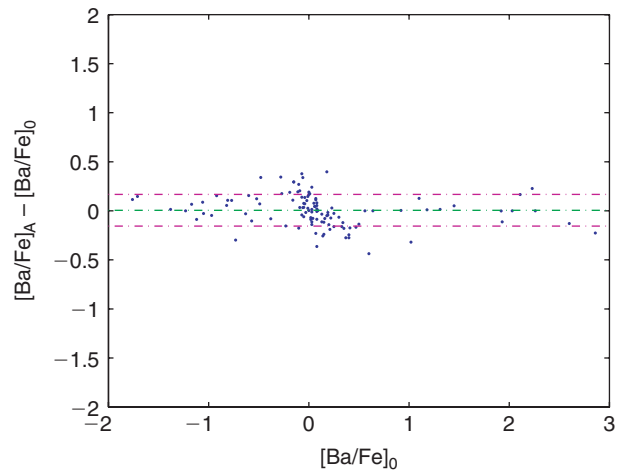


Figure 5 Distribution of the residual of the estimated [Ba/Fe] by ANN, as compared to the adopted literature values. The green line represents the mean value of the residual and the pink lines are the 1- σ lines.

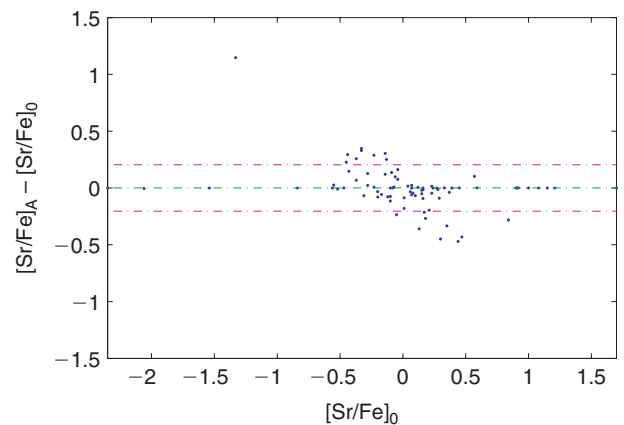


Figure 6 Distribution of the residual of the estimated [Sr/Fe], as compared to the adopted literature values. The green line represents the mean value of the residual and the pink lines are the 1- σ lines.

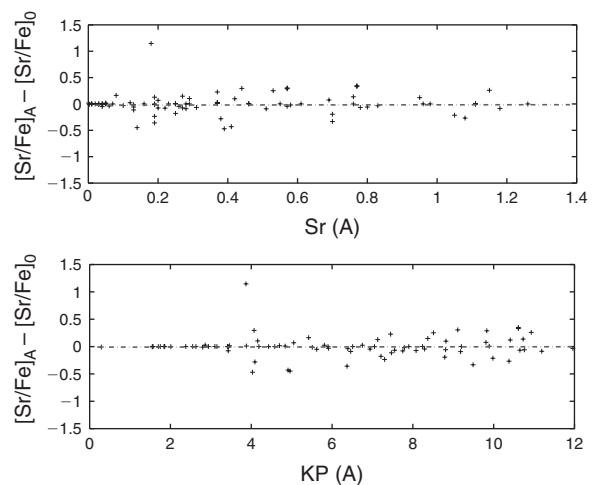


Figure 7 Distribution of the residual of the estimated [Sr/Fe] as a function of the predictor variables Sr (top panel) and KP (bottom panel).

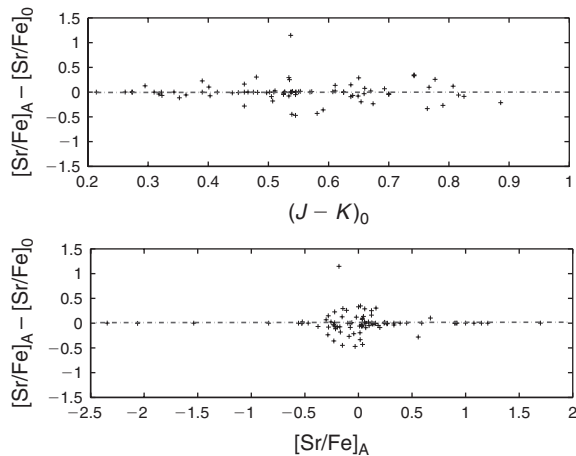


Figure 8 Distribution of the residual of the estimated $[\text{Sr}/\text{Fe}]$ as a function of the predictor variable $(J - K)_0$ (top panel) and as function of the calculated values (bottom panel).

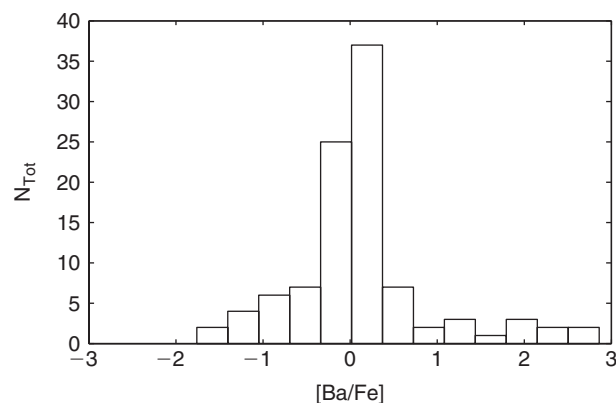


Figure 9 $[\text{Ba}/\text{Fe}]$ distribution for the calibration sample.

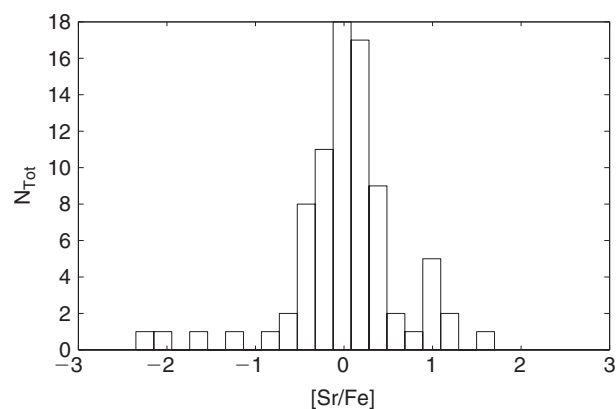


Figure 10 $[\text{Sr}/\text{Fe}]$ distribution for the calibration sample.

in Figures 9 and 10, the distributions of stars, according to barium and strontium abundance ratios, does not fill the entire parameter space. In particular, the Sr abundances fall mostly in the range $-0.5 \leq [\text{Sr}/\text{Fe}] \leq 0.5$. This is

particularly important for the ANN approach, which is not suitable for extrapolation.

After considering these limitations, we have applied only the ANN method to the program stars. The $[\text{Ba}/\text{Fe}]$ and the $[\text{Sr}/\text{Fe}]$ distributions for calibration stars can be seen in Figures 9 and 10. It appears possible to identify Ba-enhanced stars from medium-resolution data alone, with accuracy that approaches that of high-resolution investigations. Our next goal is to increase the calibration sample. There are about 100 additional stars whose Ba and Sr abundances have already estimated using high-resolution spectroscopy data by different groups, but which lack medium-resolution spectroscopy. The required follow-up of the same objects with medium-resolution ($R \sim 2000$) spectroscopy is now underway. Application of the refined estimation procedure to the program stars will appear in a forthcoming paper.

Acknowledgments

M.A.C. would like to acknowledge the L.O.C. and the Max Planck Institut für Astrophysik for making possible her attendance at the workshop. M.A.C. and S.R. thank the partial support from FAPESP, CNPq, and Capes. T.C.B. acknowledges support from the US National Science Foundation under grants AST 04–06784 and AST 07–07776, as well as from grants PHY 02–16783 and PHY 08–22648; Physics Frontier Center/Joint Institute for Nuclear Astrophysics (JINA).

References

- Adelman-McCarthy, J. K. et al., 2007, *ApJS*, 172, 634
- Allende Prieto, C. et al., 2008, *AJ*, 136, 2070.
- Beers, T. C., Preston, G. & Shectman, S., 1985, *AJ*, 90, 2089
- Beers, T. C., Preston, G. W. & Shectman, S., 1992, *AJ*, 103, 1987
- Beers, T. C., Rossi, S., Norris, J. E., Ryan, S. G. & Shefler, T., 1999, *AJ*, 117, 981
- Cayrel, R., 1988, *IAUS*, 132, 345
- Christlieb, N., 2003, *RvMA*, 16, 191
- Frebel, A., Collet, R., Eriksson, K., Christlieb, N. & Aoki, W., 2008, *ApJ*, 684, 588
- Gunn, J. E. et al., 1998, *AJ*, 116, 3040
- Lee, Y. S. et al., 2008a, *AJ*, 136, 2022
- Lee, Y. S. et al., 2008b, *AJ*, 136, 2050
- Stetson, P. B. & Pancino, E., 2008, *PASP*, 120, 1332S
- Skrutskie, M. F. et al., 2006, *AJ*, 131, 1163
- Vazdekis, A., Cenarro, A. J., Gorgas, J., Cardiel, N. & Peletier, R. F., 2003, *MNRAS*, 340, 1317
- York, D. G. et al., 2000, *AJ*, 120, 1579